Progress In Electromagnetics Research C, Vol. 122, 31–40, 2022

Stub Resonator Based Compact Low-Pass Filter (LPF) with Wide Harmonic Suppression

Arpita Mandal* **and Tamasi Moyra**

Abstract—In this article, an open T-shaped stub resonator-based compact microstrip low-pass filter (LPF) with low in-band insertion loss and wide attenuation band is proposed. The folded T-shaped stubs loaded with T-shaped open stubs are symmetrically embedded in a microstrip transmission line. The proposed LPF operates at 2.4 GHz cut-off frequency, a passband insertion loss of 0.35 dB, and a roll-off factor (ROF) of 62 dB/GHz resonated up to −48.5 dB at the filter resonant frequency. In the ground plane of the LPF, two dissimilar defected ground structures (DGSs) are placed in the array to generate additional attenuation poles for enriching the performance of the stopband. The sixth harmonic suppression is achieved with a suppression level of −20 dB up to 14.6 GHz and relative stopband rejection of 144%. The EM simulated results show a well-matched behavior with the experimental ones. The proposed LPF can be used for Bluetooth, Wi-Fi (2400 MHz), and microwave oven (2450 MHz) applications.

1. INTRODUCTION

In modern microstrip technology, microwave low-pass filters (LPFs) are crucial for removing unwanted higher frequency and inter-modulation signals. The compact size, sharp roll-off rate, low fabrication cost, and much wider rejection bandwidth are the crucial parameters for designing planar filters [1–18]. Besides, numerous techniques are presented to design low loss miniaturized LPFs [1, 2]. The lattice-shaped patches could be used with c-shaped and p-shaped resonators as suppressor units to design a wide stop bandwidth LPF [3]. However, these structures bring the problem of circuit complexity and large circuit size. In [4], open complementary split-ring resonators were proposed to meet the miniaturized LPF circuit's demand, but the circuit complexity was increased due to three-dimensional structures. The circuit size could be reduced using hairpin structures [5]. A stepped impedance hairpin resonator unit was embedded in another hairpin unit for the compact lowpass filter design with low insertion loss, but it suffered from gradual roll-off factor. To prevent this drawback, stub-based filters with compact sizes and low loss were a usual technique. [6] presented a lowpass filter designed by combining a meander line with two coupled lines, and later on, a pair of shunted open stubs were incorporated to improve the stopband performance of the filter. However, this filter suffered from large insertion loss, and also the rejection level was only −15 dB up to 10.35 GHz. The conventional structure of stepped impedance resonators is sustained by gradual cut-off frequency and poor passband response. However, modified structures [7] such as slot-back line technique [8] could improve the performance of conventional ones. A hairpin structure was centrally embedded with an m-shaped stepped impedance resonator unit for exhibiting excellent band suppression performance (40 dB out of band rejection) [9], whereas the passband response suffered from a gradual fall which resulted in a poor roll-off factor. Meanwhile, radial stubs, triangular patches, and polygonal patches were reported in designing low loss compact LPFs [10–12]. In [10], mirrored radial stubs were loaded with a c-shaped defected ground

Received 25 April 2022, Accepted 1 July 2022, Scheduled 1 August 2022
* Corresponding author: Arpita Mandal (arpitamandal108@gmail.com).
The authors are with the Department of ECE, National Institute of Technology, Agartala 799046, India.

structure etched in the ground plane, whereas in [11] polygonal resonant patches, single stair shaped stub, and open stubs were adopted forming a cascaded structure, although [11] suffered from huge insertion loss. The implementation of defected ground structures (DGS) enhanced the filter stopband performance and could mitigate the problem of circuit complexity [13–18].

This article proposes a low-loss 2.4 GHz LPF with great compactness, high selectivity, and broad stopband for S-band applications. The proposed structure is formed using horizontally aligned folded T-shaped stubs loaded with open T-shaped stubs in the high impedance line of the folded structure. An array of two dissimilar shapes of DGS has been incorporated to eliminate the higher spurious frequencies by creating additional transmission zeroes. The DGSs help to get a wideband response with an average rejection level of -20 dB up to 14.6 GHz, by not increasing the size of the filter. An FR4 substrate, which is of low cost and readily available, is used to fabricate the proposed LPF structure. The height (h) of the substrate is 1.6 mm having a loss tangent ($\tan\delta$) of 0.02 and dielectric constant (ε_r) of 4.4. The lumped circuit of the proposed LPF is also derived and simulated. The electromagnetic simulated, circuit and measured responses show a well-matched behavior among each other. In the last section, the proposed structure is compared with the previous related works. Table 1 displays the parametric analysis of basic parameters for various L_t values, and likewise, the effect of filtering parameters by changing the coupling gap (G) is represented in Table 2. The formula for calculating the roll-off factor is discussed in the subsequent subsection. The tabulated data shows that the optimum result is obtained for $L_t = 6.88$ mm and $G = 0.625$ mm.

Table 1. Parametric variation for various L_t values.

L_t (mm)	Roll-off Factor (dB/GHz)	Suppression Level (dB)
8.88	56.85	−38.25
7.88	58.71	−41.75
7.28	60	−45
6.88	62	−48.5

Table 2. Parametric variation for various values of G.

G (mm)	f_c (GHz)	Insertion loss (dB)	Roll-off Factor (dB/GHz)
0.125	2.36	0.45	62.81
0.375	2.39	0.42	62.42
0.625	2.4	0.36	62
0.825	2.38	0.37	60.12

2. FILTER DESIGN AND ANALYSIS

2.1. Microstrip Realization

The design and analysis of the filter are initiated from the comparative analysis of a generalized third-order Chebyshev LPF response. The folded T-shaped stub, consisting of a high impedance transmission line and a low impedance folded section, is aligned horizontally and connected to the 50 Ω microstrip line. The performance of the filter is enhanced significantly in terms of insertion loss and sharp fall rate by the introduction of a T-shaped stub in the existing structure. The high impedance line of the T-shaped open stub is loaded symmetrically on the high impedance line of the folded structure to improve the performance of the filter and to create transmission zeroes. Due to this, a coupling gap (G) is created between the open-ended arm of the T-shaped stub and the horizontal arm of the folded stub. Finally, the modified stub resonator (Figure 1(a)) is formed for achieving lowpass filtering response, and further analysis of the modified structure based on its performances is studied. Figure 1(b) shows that

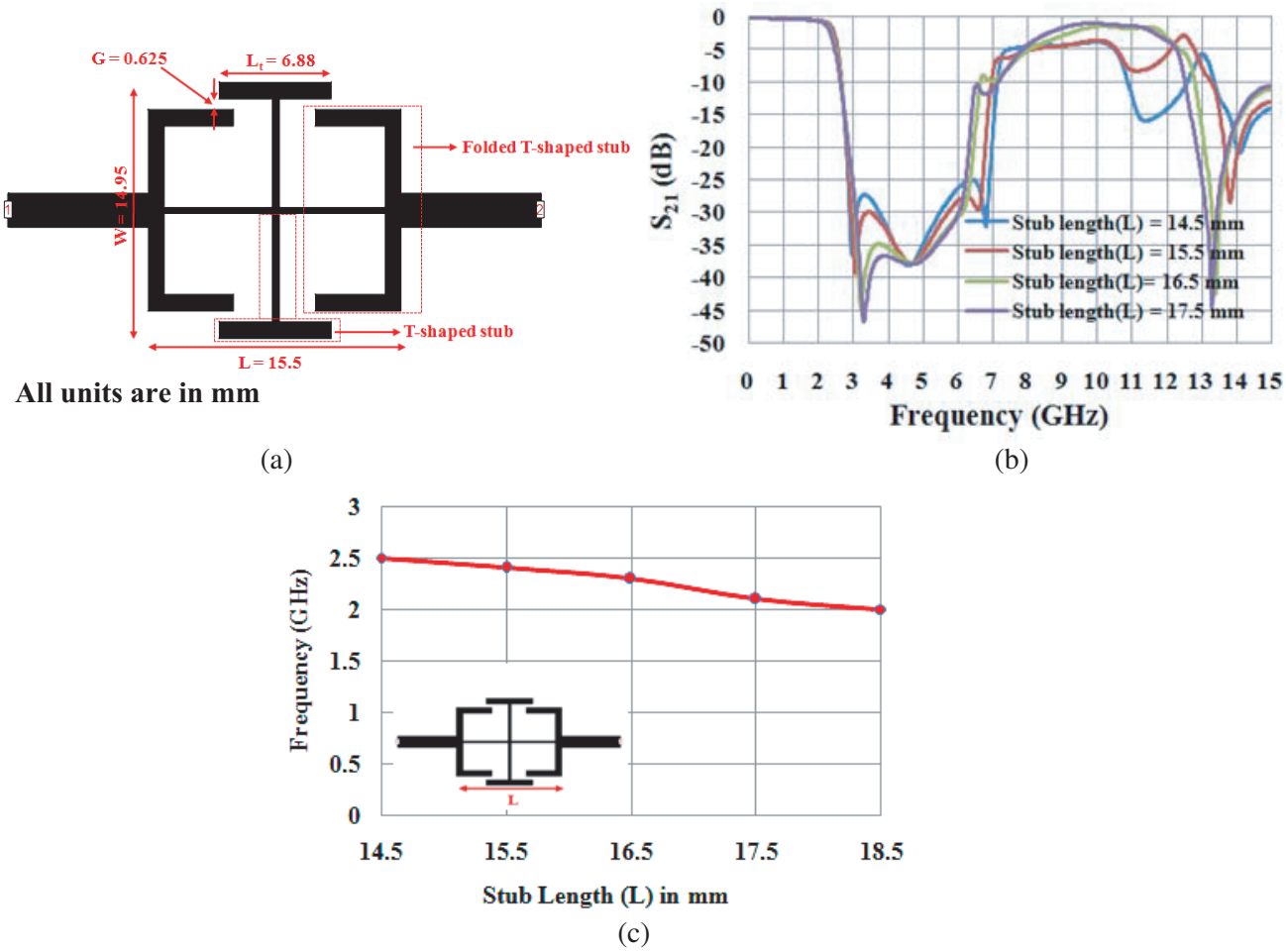

Figure 1. Modified stub resonator. (a) Physical outlook. (b) Frequency simulated responses for different stub lengths. (c) Deviation of cut-off frequency vs stub lengths.

different operating frequencies are obtained by tuning the length (L) of the folded T-shaped stub, and the deviation of stub length (L) for different values of the cut-off frequency is depicted in Figure 1(c). 'L_t' denotes the length of the T-stub, and 'W' is the width of the modified stub resonator. Similarly, the optimum requirement is achieved by performing the parametric study of other values. Table 1 displays the parametric analysis of basic parameters for various L_t values, and likewise, the effect of filtering parameters by changing the coupling gap (G) is represented in Table 2. The formula for calculating the roll-off factor is discussed in the subsequent subsection. The tabulated data shows that the optimum result is obtained for $L_t = 6.88$ mm and $G = 0.625$ mm.

2.2. Analysis of Defected Ground Structures

The dumbbell-shaped DGS unit shown in Figure 2(a) presents a narrow slot connected to two rectangular patches on either side and is etched in the ground plane. It has been found that the variation of resonant frequency can be performed by changing the physical dimensions of etched rectangular patches. However, wide harmonic suppression with reduced circuit size is a major concern for patterned ground structures. For that, three dumbbell DGSs are etched in array to create three resonant frequencies, and the resultant provides wide stopband keeping the DGS cell size unaltered. Furthermore, the dumbbell patterned ground structure is modified to reduce the cell size and achieve higher resonant frequency simultaneously. The slot of the dumbbell DGS is moved to the edges, and it is lengthened across the etched rectangular patches. The width of the patches is decreased, and a patch of similar dimension is

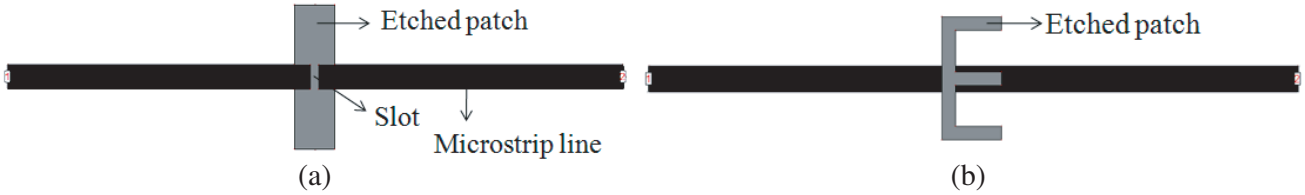

Figure 2. DGS structure. (a) Dumbbell-shape. (b) E-shape.

inserted in the middle of each etched pattern parallely, forming an E-shape. The E-shaped DGS unit is depicted in Figure 2(b). The shield current distribution in the ground plane is affected using these DGS structures. The electrical path length is increased, which introduces an additional inductance, and due to charge accumulation across the etched defects, a capacitive effect is induced. Hence, one DGS unit cell creates one LC tank circuit and provides one transmission zero which is explained in the following section in detail.

2.3. Frequency Simulated Responses

The design procedure of the proposed LPF is illustrated in its subsequent steps and depicted in Figures 3(a)–(e) chronologically. Initially, the response of the folded T-shaped symmetrical stub is observed (Figure 3(a)). Later on, the high impedance line is loaded with an open-ended T-shaped stub, forming the modified stub resonator, to improve the filter performance (Figure 3(b)). The desired cut-off frequency is found at 2.4 GHz, and the transmission zeroes can be obtained between 3.05 GHz and 6.60 GHz (Figure 3(b)). For widening the stopband width with improved passband response, the DGSs are etched from the metallic ground plane to introduce a small amount of capacitance and extra inductance in the microstrip transmission line. In the ground plane, a unit dumbbell-shape and E-shape DGSs cells (Figure 3(c)) are introduced to obtain a bandstop characteristic with gradual fall at 7.5 GHz and 9.8 GHz, respectively. The DGSs increase the mutual coupling with the microstrip line and suppress the higher harmonics. The harmonics of the proposed filter are suppressed up to 14.6 GHz using an array of dumbbell shape DGSs and E shape DGSs with an average rejection level of −20 dB throughout the stopband. The insertion loss, roll-off factor, and relative stop bandwidth of the proposed LPF are 62 dB/GHz, 0.35 dB, and 144%, respectively. The schematic outlook is given in Figure 3(d) (signal plane) and Figure 3(e) (ground plane) of the proposed design. The electromagnetic simulation response of the filter is examined and displayed in Figure 3(f). The equivalent LC circuit model of the designed filter is discussed in Section 4.

2.4. Filter Characteristics

The sharpness of roll-off is obtained as

$$\xi = \frac{\alpha_{\max} - \alpha_{\min}}{f_s - f_c} \ \text{dB/GHz} \tag{1}$$

where the 40 dB attenuation point is signified by "α_{max}", and the 3 dB attenuation point is denoted by "α_{min}". The 3 dB cut-off frequency is denoted by "f_c", and the 40 dB stopband frequency is signified by "f_s". The roll-off rate of 62 dB/GHz with −48.5 dB attenuation at the filter resonant frequency is obtained. The relative stop bandwidth (RSB) of the proposed LPF can be found as

$$\text{RSB} = \frac{\text{Stop bandwidth}}{\text{Stopband center frequency}} \tag{2}$$

where 144% is the RSB. The suppression factor is defined as suppression/10 dB which is attained on the basis of average stopband suppression and is approximately considered as 2. The size of the filter can be given as

$$\text{NCS} = \frac{\text{Physical size (length} * \text{width)}}{\lambda_g^2} \tag{3}$$

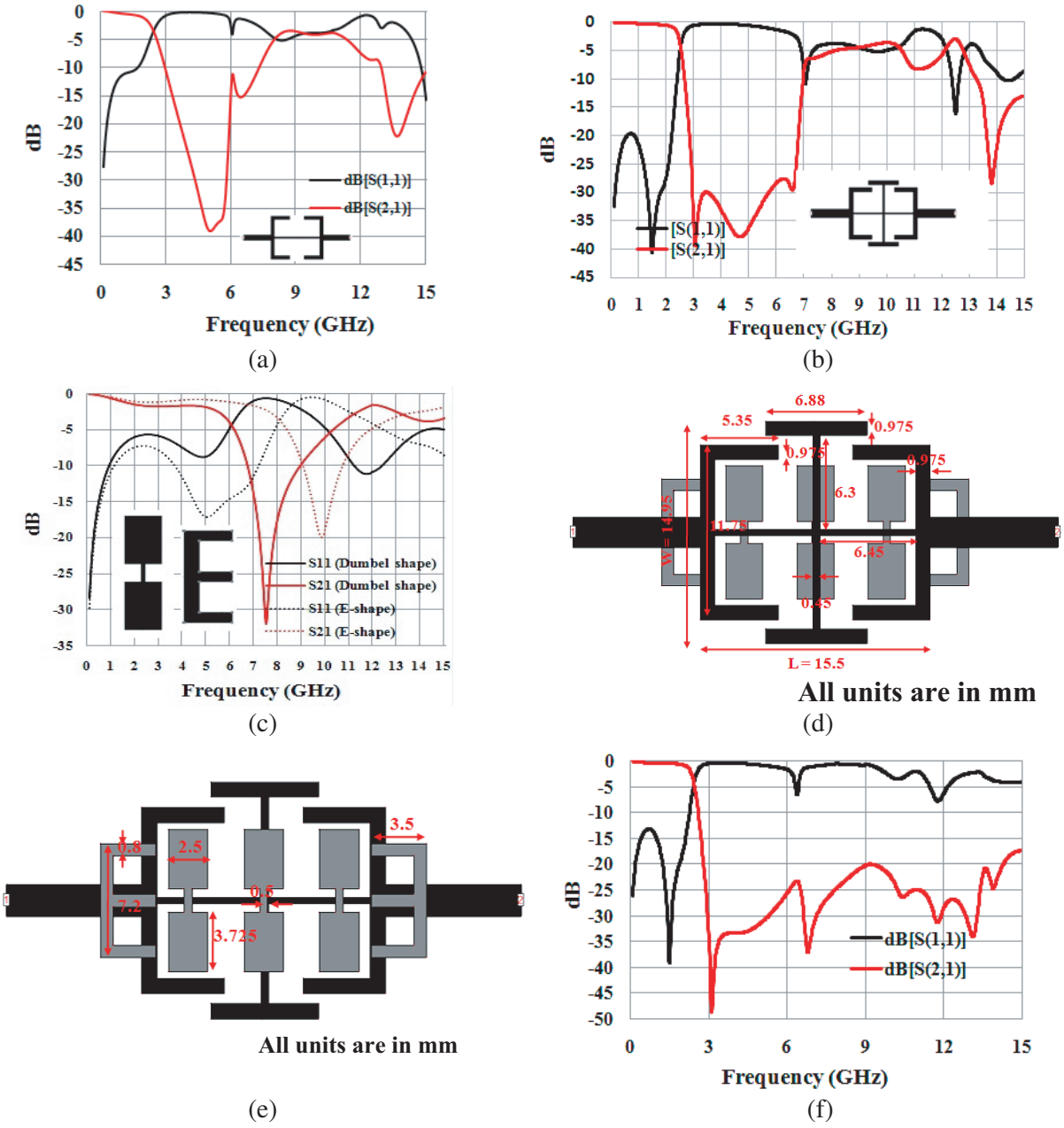

Figure 3. (a) Scattering parameters of Folded T-shaped stub. (b) Scattering parameters of Modified stub resonator. (c) Responses of DGS. (d) Proposed LPF signal plane metallic view. (e) View of the ground plane. (f) Proposed LPF EM frequency simulated responses in dB.

The normalized circuit size (NCS) of the filter is $(0.05\lambda_g^2)$. The formula for calculating figure of merit (FOM) is given as

$$\text{FOM} = \frac{\text{RSB} \times \xi \times \text{SF}}{\text{AF} \times \text{NCS}} \tag{4}$$

where AF stands for the circuit complexity factor or architecture factor. The FOM of the filter is 4464.

2.5. Current Distribution and Group Delay

The distributions of current of the proposed design at various conditions around cut-off frequencies are examined using Zealand IE3D Electromagnetic software and depicted in Figure 4. The current vector distributions of the LPF at 1.24 GHz, 2.41 GHz, 2.8 GHz, and 5.74 GHz are investigated. It gives equal input and outputs current distribution at a cut-off frequency (2.4 GHz), while its amplitude is diminished at higher frequencies (5.8 GHz). Furthermore, due to the DGSs structures in the ground plane, the effective current conducting path is increased, and the current density in the signal plane is enhanced. It is observed that the current distribution is minimum at the cut-off frequency 2.4 GHz (Figure 4(f)), since it becomes exactly negative of the top plane.

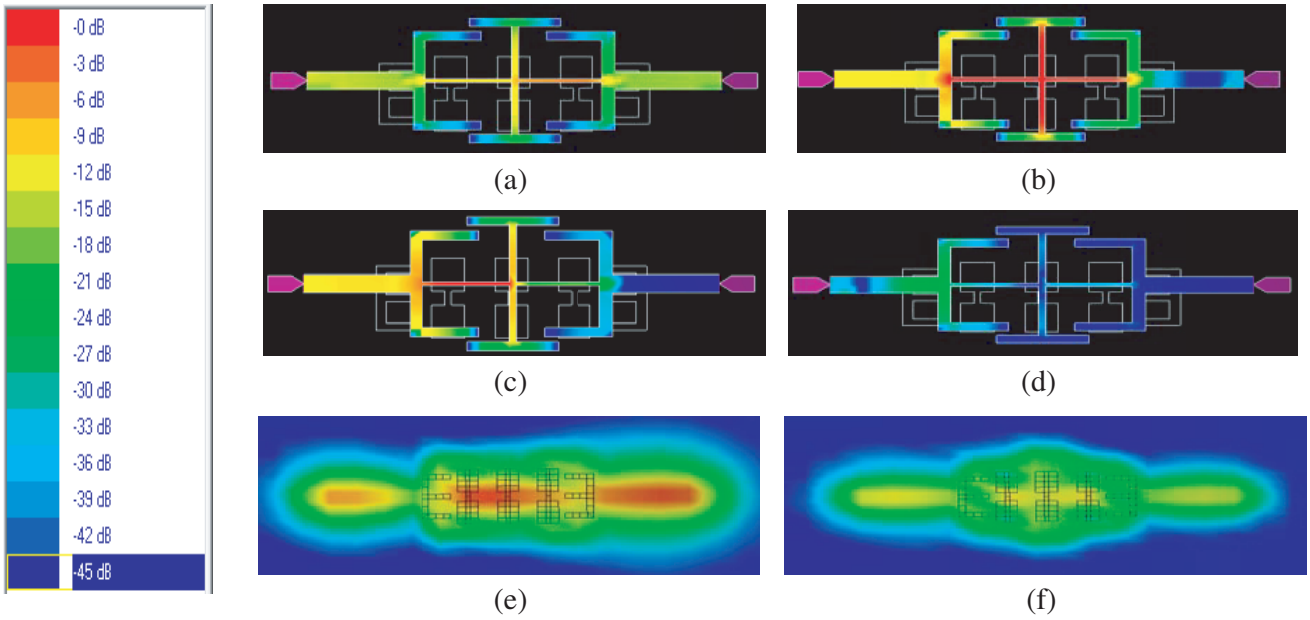

Figure 4. LPF current distributions at (a) 1.24 GHz, (b) 2.41 GHz, (c) 2.8 GHz, (d) 5.74 GHz. (e) Ground plane at 1.3 GHz. (f) Ground plane at 2.4 GHz.

The filter order is nearly proportional to group delay (GD) and is defined as the measure of phase distortion. The standard equation to calculate GD may be written as

$$\text{Group Delay} = -\frac{\Delta\phi}{\Delta\omega} \tag{5}$$

where the angular frequency is represented by "ω" in rad/sec that is equal to $2\pi f$, and "ϕ" is the S_{21} phase angle. The GD in average obtained in the passband region is 0.46 ns and is depicted in Figure 5.

3. MEASUREMENT RESULTS

The proposed LPF is fabricated on FR4, and the Vector Network Analyzer (VNA) N5221A is used to measure the performance of the fabricated prototype. The graph of the measured response presents an LPF having in-band loss (0.5 dB) with a sharp fall rate of 63 dB/GHz, the figure of merit 4127, and broader stopband characteristics (RSB of 131%) with highly selective performance. It has been found that the scattering parameters of measured and EM simulated responses show good similarity with each other. The experimental vs simulated result is represented in Figure 6(c), and the average suppression of harmonics (measured) is achieved almost up to −20 dB from 3.13 GHz (resonant frequency) to 15 GHz. The proposed LPF has considered the suppression factor (SF) as 2. The 50-ohm microstrip line is excited by the input and output excitation ports for perfect matching. Figure 6(a) and Figure 6(b) depict the pictorial view of the fabricated structures, respectively.

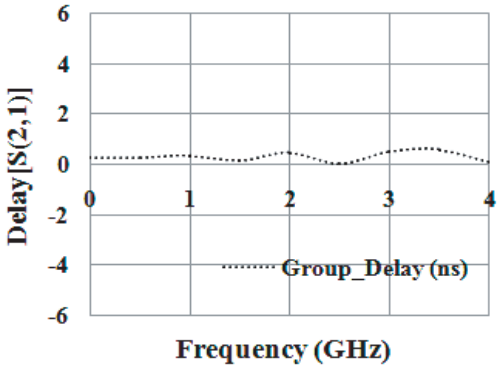

Figure 5. LPF group delay.

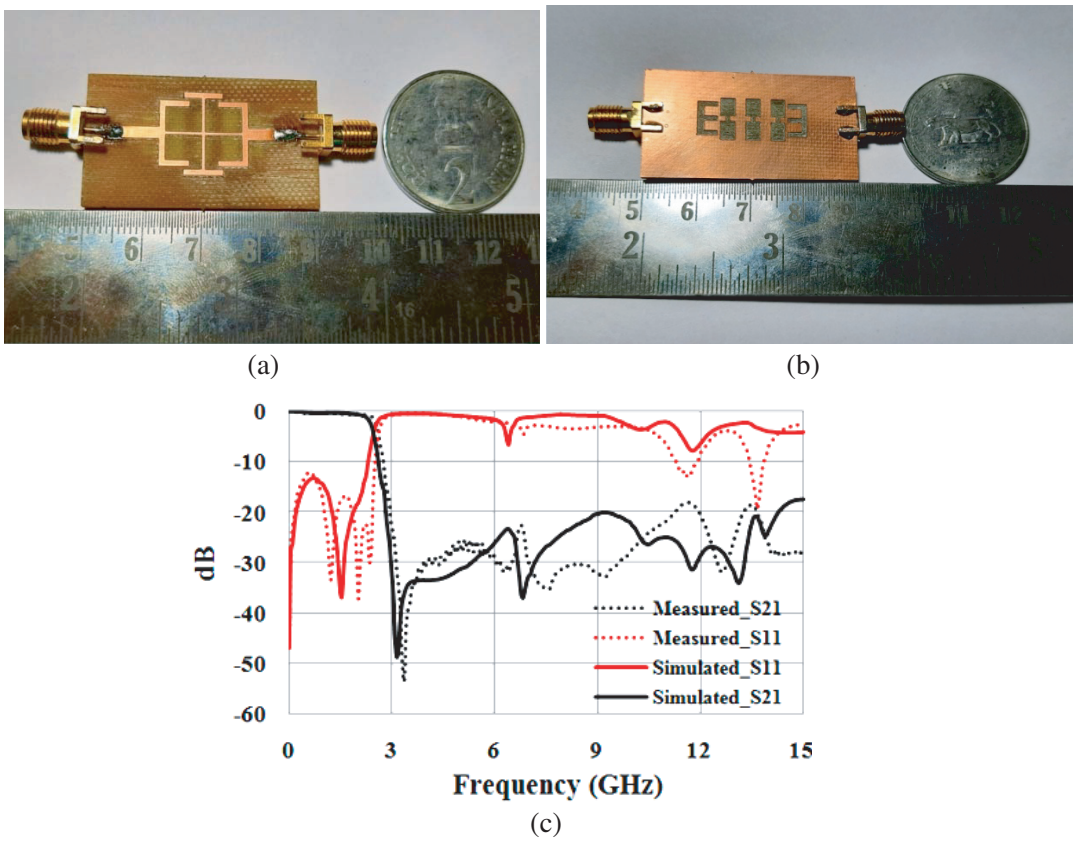

Figure 6. Fabricated prototype. (a) Layout of the Signal plane. (b) View of the ground plane. (c) Measured vs EM frequency simulated result.

4. EQUIVALENT CIRCUIT OF THE PROPOSED LPF

The LC circuit of the proposed filter shown in Figure 7(a) is extracted from the structure, and the circuit modeling is performed using Advanced Design System (ADS) software. C_3 is the parasitic capacitance, and L_2 is the high impedance transmission line inductance. The incorporation of DGSs in the existing structure provides inductance and capacitance, producing an LC tank circuit and is defined as [19]

$$L_g = \frac{1}{4\pi^2 f_o^2 C_g} \tag{6}$$

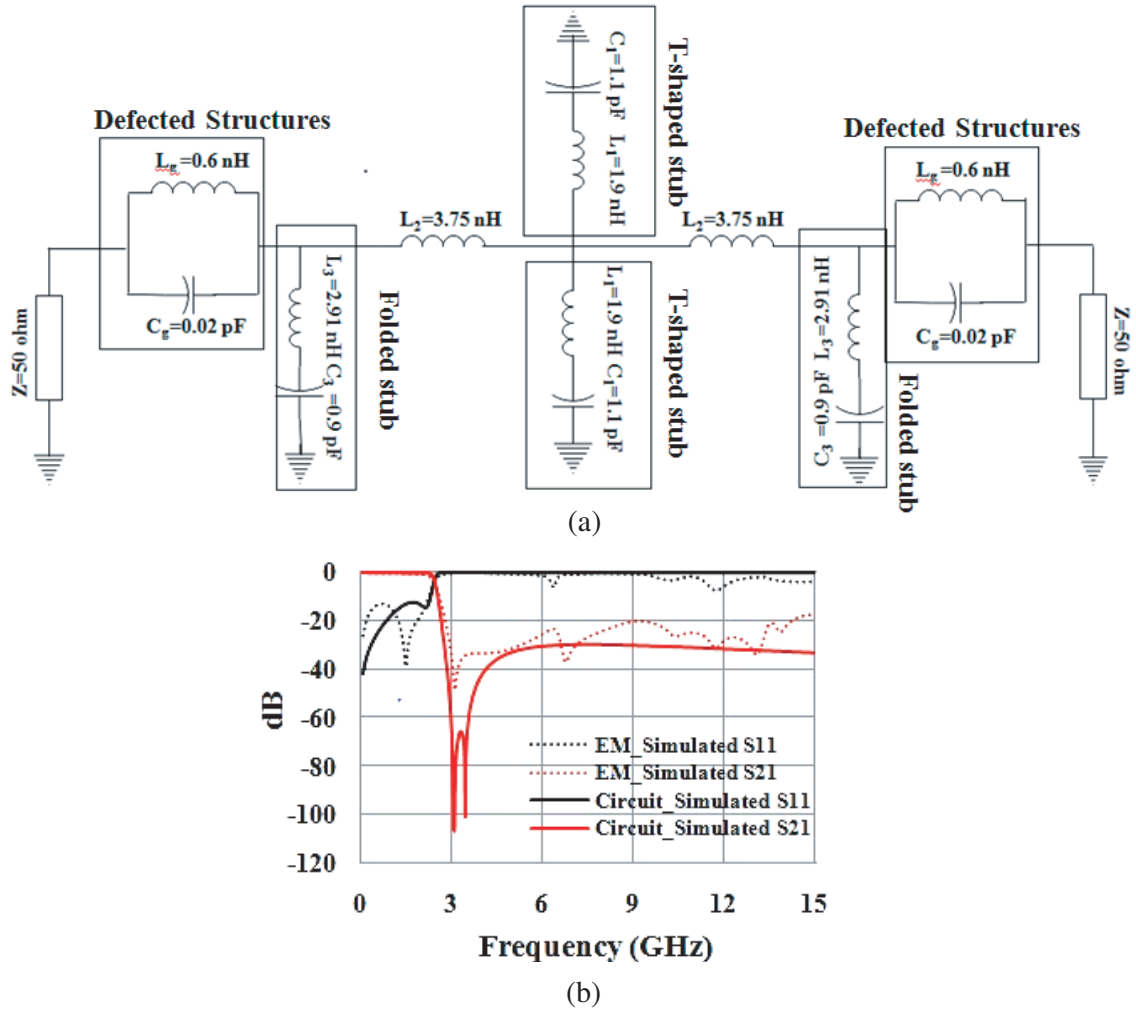

Figure 7. Proposed LPF. (a) Lumped equivalent circuit. (b) Circuit vs EM simulated result.

$$C_g = \frac{f_c}{4\pi Z_o \left(f_o^2 - f_c^2\right)} \tag{7}$$

The circuit simulated vs EM simulated responses are displayed in Figure 7(b), and it provides low in-band loss and a sharp roll-off factor. Since the accurate values of the lumped elements are difficult to extract, some mismatch arises between the circuit simulated and EM simulated results. Moreover, this deviation may be due to connector loss and substrate imperfection.

The performance comparison between the previously related LPFs and the newly proposed work is made accordingly in Table 3. In [6], and [12], the filter provides the least circuit size but endures poor roll-off rate [7]. Similarly, [9] has the lowest insertion loss with excellent band rejection compared with others presented in the table despite poor stopband performances. [12] and [15] have a good band suppression level with high relative stop bandwidth but suffer from large insertion loss. Furthermore, the proposed LPF is fabricated on a low-cost FR4 substrate, but a costlier substrate is used for the other works except [13]. This provides the proposed design an additional advantage. Hence based on Table 3, the proposed LPF is economical with a wide stopband and the highest roll-off rate.

Table 3. Performance comparison table.

References	Substrate Used	f_c (GHz)	Insertion Loss in passband (dB)	ξ (dB/GHz)	RSB	Band suppression level and Attenuation band	NCS (λ_g^2)
[6]	Roger RO4350	1.2	NA	17	1.58	−15 dB up to 10.35 GHz	0.0095
[7]	RO4003	2.85	0.3	7.17	1.32	−20 dB up to 6.3 GHz	0.046
[9]	Roger RO4003C	1.8	0.25	45.12	1.33	−40 dB up to 13 GHz	0.02
[12]	Roger RO4003C	1	0.4	37	1.65	−20 dB up to 14.3 GHz	0.009
[13]	FR4	2.4	0.35	36	0.86	−20 dB up to 6 GHz	0.07
[14]	RO4003	1.4	0.3	22.5	0.98	−20 dB up to 6.5 GHz	0.15
[15]	Roger RO 4003	2.4	0.8	37.2	1.62	−30 dB up to 9.8 GHz	0.0378
Proposed work	FR4	2.4	0.35	62	1.45	−20 dB up to 14.6 GHz	0.05

5. CONCLUSION

A loaded open stub resonator is proposed to design a compact, sharp rejection characteristic, low-cost LPF with wide attenuation band. T-shaped open stub resonators are loaded along the folded structure high impedance transmission line to enhance the performance of the filter. Two dissimilar shapes of DGS are introduced to suppress the higher spurious harmonics for widening stopband characteristics. The proposed filter is theoretically analyzed, fabricated, and finally measured for experimental validation. The equivalent lumped circuit of the LPF is derived. The benefits such as compact structure (15.5 mm × 14.95 mm), good roll-off rate (62 dB/GHz), low insertion loss (0.35 dB), and wide stopband with −20 dB attenuation up to 14.6 GHz are attained for the proposed 2.4 GHz LPF, and the filter may be suitable for applications in Bluetooth, Wi-Fi (2.4 GHz), and microwave oven (2.45 GHz).

ACKNOWLEDGMENT

The authors are very thankful to ISRO project for their support.

REFERENCES

1. Hammed, R. T., S. H. Hassan, and S. L. Ajeel, "New compact Low-Pass Filter (LPF) using cascaded square open loop resonator," *International Journal of Electronics and Communications (AEU)*, Vol. 92, 93–97, 2018.
2. Hiedari, B. and F. Shama, "A harmonics suppressed microstrip cell for integrated applications," *International Journal of Electronics and Communication (AEU)*, Vol. 83, 519–522, 2018.

3. Hayati, M., M. Ekhteraei, and F. Shama, "Compact lowpass filter with flat group delay using lattice-shaped resonator," *Electronics Letters*, Vol. 53, No. 7, 475–476, 2017.
4. Karthikeyan, S. S. and R. S. Kshetrimayum, "Compact and wide stopband lowpass filter using open complementary split ring resonator and defected ground structure," *Radio Engineering*, Vol. 24, No. 3, 708–711, 2015.
5. Liu, S., J. Xu, and Z. Xu, "Compact lowpass filter with wide stopband using stepped impedance hairpin units," *Electronics Letters*, Vol. 51, No. 1, 67–69, 2015.
6. Chen, X., L. Zhang, Y. Peng, Y. Leng, H. Lu, and Z. Zheng, "Compact lowpass filter with wide stopband bandwidth," *Microwave and Optical Technology Letters*, Vol. 57, No. 2, 367–371, 2015.
7. Ellatif, W. A. and A. Boutejdar, "Design of low-pass filter using meander inductor and U-form Hi-Lo topology with high compactness factor for L-band applications," *Progress In Electromagnetics Research M*, Vol. 55, 95–107, 2017.
8. Huang, S. Y. and Y. H. Lee, "Compact stepped-impedance lowpass filter with a slot-back microstrip line," *Microwave and Optical Technology Letters*, Vol. 50, No. 4, 1059–1061, 2008.
9. Du, Z., H. Yang, H. Zhang, and M. Zhu, "Compact lowpass filter with high suppression level and wide stop-band using stepped impedance m-shape units," *Microwave and Optical Technology Letters*, Vol. 56, No. 12, 2947–2950, 2014.
10. Kchairi, A. B., M. Boussouis, and N. A. Touhami, "High-performance LPF using coupled C-shape DGS and radial stub resonators for microwave mixer," *Progress In Electromagnetics Research Letters*, Vol. 58, 97–103, 2016.
11. Rekha, T. K., P. Abdulla, P. M. Raphika, and J. P. Muhammed, "Compact microstrip lowpass filter with ultra-wide stopband using patch resonators and open stubs," *Progress In Electromagnetics Research C*, Vol. 72, 15–28, 2017.
12. Wang, J., H. Cui, and G. Zhang, "Design of compact microstrip lowpass filter with ultra-wide stopband," *Electronics Letters*, Vol. 48, No. 14, 854–856, 2012.
13. Sen, S., T. Moyra, and D. Sarkar, "Modelling and validation of microwave LPF using modified rectangular Split Ring Resonators (SRR) and defected structures," *AEU — International Journal of Electronics and Communications*, Vol. 88, 1–10, 2018.
14. Boutejdar, A. and W. A. E. Ali, "Improvement of compactness of low pass filter using new quasi Yagi-DGS-resonator and multilayer-technique," *Progress In Electromagnetics Research C*, Vol. 69, 115–124, 2016.
15. Huang, S. Y. and Y. H. Lee, "A compact E-shaped patterned ground structure and its applications to tunable bandstop resonator," *IEEE Transactions on Microwave Theory and Techniques*, Vol. 57, No. 3, 657–665, 2009.
16. Shi, L.-F., Z.-Y. Fan, and D. J. Xin, "Miniaturized low-pass filter based on defected ground structure and compensated microstrip line," *Microwave Optical Technology Letters*, Vol. 62, No. 3, 1093–1097, 2019.
17. Mandal, A. and T. Moyra, "Stepped Impedance Hairpin Resonator (SIHR) based compact lowpass filter with wide attenuation band," *Electromagnetics*, Vol. 42, No. 1, 2022.
18. Choudhary, D. K. and R. K. Chaudhary, "Compact lowpass and dual-band bandpass filter with controllable transmission zero/center frequencies/passband bandwidth," *IEEE Transactions on Circuits and Systems II: Express Briefs*, Vol. 67 No. 6, 1044–1048, 2020.
19. Hong, J.-S. and M. J. Lancaster, *Microstrip Filters for RF/Microwave Applications*, 157–158, John Wiley & Sons, Inc, 2001.